ISSN 0020-4412, Instruments and Experimental Techniques, 2016, Vol. 59, No. 3, pp. 425–432. © Pleiades Publishing, Ltd., 2016.
Original Russian Text © A.N. Babitskii, B.A. Belyaev, N.M. Boev, G.V. Skomorokhov, A.V. Izotov, R.G. Galeev, 2016, published in Pribory i Tekhnika Eksperimenta, 2016, No. 3, pp. 96–104.

GENERAL EXPERIMENTAL TECHNIQUES

A Magnetometer of Weak Quasi-Stationary and High-Frequency Fields on Resonator Microstrip Transducers with Thin Magnetic Fields

A. N. Babitskii[a], B. A. Belyaev[a, b, c]*, N. M. Boev[a, b], G. V. Skomorokhov[a], A. V. Izotov[a, b], and R. G. Galeev[d]

[a] *Kirensky Institite of Physics, Siberian Branch, Russian Academy of Sciences, Akademgorodok 50, str. 38, Krasnoyarsk, 660036 Russia*
[b] *Siberian Federal University, pr. Svobodnyi 79, Krasnoyarsk, 660036 Russia*
[c] *Reshetnev Siberian State Aerospace University, pr. Im. Gazety Krasnoyarskii rabochii 31, Krasnoyarsk, 660014 Russia*
[d] *OAO NPP Radiosvyaz', Krasnoyarsk, 660021 Russia*
**e-mail: belyaev@iph.krasn.ru*

Received April 14, 2015; in final form, July 20, 2015

Abstract—A high-sensitivity magnetometer for simultaneous measurements of three components of a weak quasi-stationary or high-frequency magnetic-field vector was developed and investigated. Microstrip structures that are based on irregular resonators serve as the magnetometer transducers. An anisotropic thin-film magnetic structure is used as the sensing element. This structure consists of two thin magnetic films that are prepared by magnetron sputtering of a $Ni_{75}Fe_{25}$ permalloy target and separated by a silicon monoxide layer. It is demonstrated that the transducer exhibits the maximum sensitivity, when the easy magnetization axis of the film structure is orthogonal to the polarization direction of the pumping microwave magnetic field in the microstrip resonator and at an optimal value of a constant magnetic bias field and its optimal deflection from the pumping-field polarization direction which is parallel to it. The magnetometer is characterized by a wide dynamic range of measured magnetic fields, 10^{-10}–10^{-4} T, and a wide frequency range, 10^{-1}–10^{5} Hz.

DOI: 10.1134/S0020441216030131

INTRODUCTION

High-sensitivity magnetometers of weak quasi-stationary magnetic fields are intended for solving numerous scientific and technological problems, primarily the geomagnetometry problems that are associated with both studies of the geological structure of the earth and exploration activity [1–3] and archeologic investigations [4, 5]. Sensors of weak magnetic fields are used in medicine [6], burglar alarms, and special instruments, which are used in space technologies [7] and other fields. In view of the great need of such devices, it is important that the latter would have not only a required sensitivity but also be simple in manufacture and have acceptable mass–size and energy characteristics, high reliability, and a relatively low cost in mass production.

As is known, SQUID magnetometers have the lowest sensitivity threshold, $\sim 10^{-15}$ T [6], but they are complex, expensive, power-consuming, and bulky devices. Liquid helium is used to provide cryogenic temperatures in them; therefore, these devices are not suitable for operation under field conditions. Other quantum-magnetometry methods that are based on the high stability of the energy of the standard transitions between long-lived atomic states are also promising in metrology of the magnetic-field strength [8]. These methods also have a record-level high sensitivity, but instruments on their basis can be successfully used only when solving special problems from a comparatively narrow range.

Easy-to-operate fluxgate magnetometers have become widespread [9], although their threshold sensitivity is much lower and reaches $\sim 10^{-10}$ T. It is important to note that the upper limit of the operating-frequency band of fluxgates is only several kilohertz, but in some applications, e.g., in pulse electrical prospecting with the artificial excitation of a medium, magnetometers must have an operating-frequency band of several tens of kilohertz [10]. Therefore, the development and investigation of novel designs of broadband high-sensitivity magnetometers are important and urgent problems. In this case, researchers pay special attention to vector magnetometers that are able to register not only the magnitude of the measured field but also its direction.

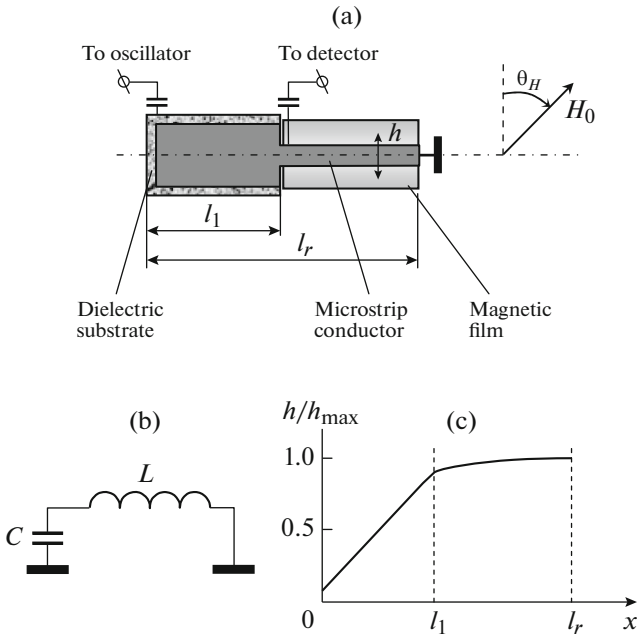

Fig. 1. (a) A microstrip resonator with a thin magnetic film, (b) its equivalent circuit, and (c) the distribution of the high-frequency current amplitude along the length of the resonator conductor.

The comparatively narrow operating-frequency band of both fluxgate magnetometers and conventional magnetometers that are based on thin magnetic films (TMFs) [10–12] is determined by the use of inductive sensitive elements—magnetic-field sensors—in them. In inductive sensors, the high-frequency pumping and signal picking-off are performed with coils that are wound directly on a core of a soft magnetic material or on a substrate with a TMF deposited on it. It is obvious that in such structures, the coil windings shield external high-frequency magnetic fields, thus substantially lowering the upper frequency-band edge of magnetometers. Thin-film sensors in the form of microstrips are deprived of these disadvantages and are also more manufacturable [13–15].

This paper presents the results of investigations of a vector magnetometer that is based on microstrip resonance structures, which contain TMFs, and satisfies the state-of-the-art requirements.

MAGNETIC-FIELD SENSOR BASED ON A MICROSTRIP RESONATOR WITH A THIN MAGNETIC FIELD

Let us consider the structure of an irregular quarter-wavelength microstrip resonator (MSR) that consists of two sections of strip transmission lines, one of which has a low characteristic impedance, and the impedance of the other is high. In this case, the stripline conductor of the resonator with the length l_r consists of two regular sections (Fig. 1a). The wide conductor of the low-resistance section with the length l_1 is deposited on a substrate with a high relative permittivity. One of its ends is free, and the other is connected to the narrow conductor of the high-resistance section of an asymmetric air stripline. The other end of the conductor is connected to the shield.

The equivalent circuit of the resonator is a parallel oscillatory circuit (Fig. 1b), in which a transmission-line section with a low characteristic impedance was used as the capacitance, and a section with a high characteristic impedance served as the inductance. The magnetic film that is produced on its substrate is positioned under the narrow conductor of the MSR at the location of an antinode of the microwave magnetic field h. The amplitude distribution of this field along the entire conductor length is shown in Fig. 1c.

As is known, irregular microstrip resonators are widely used not only in the structures of band-pass filters [16], but also as measuring cells for studying the dielectric characteristics of materials (e.g., liquid crystals) at microwaves [17]. Irregular MSRs may also serve as sensors of weak quasi-stationary or high-frequency magnetic fields [18]. In this case, the resonator that contains a TMF is connected via capacitive coupling to the input and output ports (see Fig. 1a). The points for connecting the ports to the strip conductor may be chosen arbitrarily because the input and output ports are matched to the leading-in high-frequency transmission lines by selecting the coupling capacitances.

In this case, as the distance between the point of connection of any port to the free end of the MSR's wide conductor, where the high-frequency voltage antinode is located, decreases, the optimal value of the corresponding coupling capacitances decreases as well. The pump oscillator that operates at the MSR resonance frequency is connected to the input port, and a microwave detector that yields a useful signal is connected to the output port. A signal is formed owing to a shift of the resonance frequency and a change in the resonator quality factor upon a change in the magnetic permeability of the TMF under the action of the measured magnetic field, i.e., according to the same scheme as in conventional fluxgate magnetometers on the basis of oscillatory circuits with TMFs [10].

It should be noted that in order to increase the sensitivity of a sensor, it is desirable to use multilayer magnetic structures possessing a uniaxial magnetic anisotropy in their plane, as in film magnetometers on oscillatory circuits with TMFs [10]. As a rule, such structures are manufactured via vacuum evaporation of metal magnetic films with a thickness of about one skin layer, which are separated by dielectric interlayers that exclude an electric contact between TMFs. This is necessary for reducing the microwave-power losses that are related to eddy currents.

In the investigated sensor, we used a magnetic film structure that consisted of only two permalloy TMFs

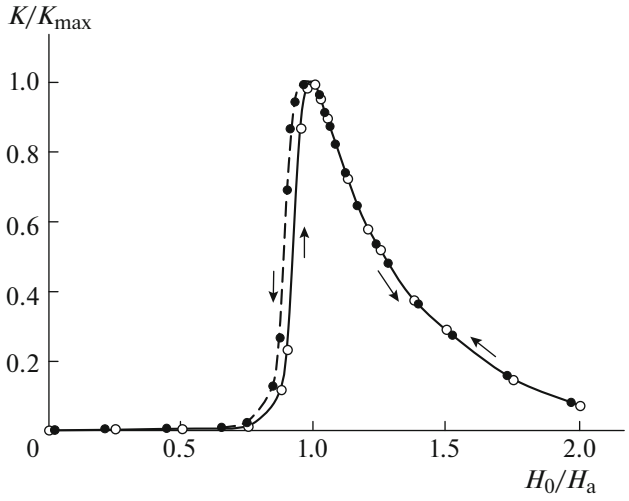

Fig. 2. The dependences of the conversion coefficient, which is normalized to its maximum value, on the bias magnetic field, which is normalized to the uniaxial magnetic-anisotropy field. Light and dark dots show the forward and backward traces of the magnetic field.

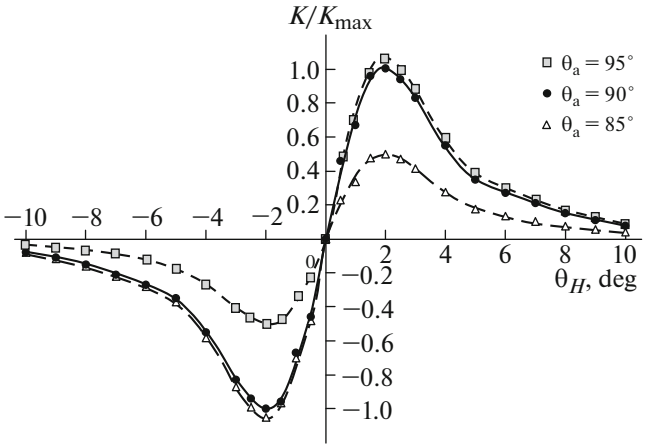

Fig. 3. The dependences of the normalized conversion coefficient of the microstrip sensor on the direction angle of the bias magnetic field for three orientation angles of the TMF easy-magnetization axis relative to the high-frequency field polarization.

with a thickness of 0.15 μm each, which were separated by a 0.5-μm-thick silicon monoxide layer. To be protected against the atmosphere, the film structure was also coated with a 0.5-μm-thick silicon monoxide layer. The magnetic films were obtained via magnetron sputtering of a $Ni_{75}Fe_{25}$ target onto CT-50 glassceramic substrates of standard dimensions, 60 × 48 mm^2, and a thickness of 0.5 mm, which were preliminarily coated with a 0.5-μm-thick silicon monoxide layer for "curing" irregularities on the substrate surface.

The uniaxial magnetic anisotropy, which is characterized by a field H_a with a typical small value of 4–8 Oe, was induced in the TMF by a constant uniform magnetic field of ~200 Oe that was applied in the substrate plane during the evaporation. It is obvious that the easy magnetization axis (EMA) of the thus manufactured film structure is positioned in its plane and coincides with the direction of the magnetic field that is applied during the TMF evaporation. Note that the magnetic moments of the films in the absence of external magnetic fields are oriented in the EMA direction.

In the investigated sensor, a section of the low-resistance transmission line with a 5-mm-long conductor with a width of 4 mm was manufactured on a 0.5-mm-thick thermostable high-frequency B-80 ceramic substrate. Its relative permittivity was $\varepsilon = 80$. A magnetic film structure with an area of ~5 × 4 mm^2 was positioned under the conductor of an air high-resistance line with a 0.5-mm-wide and 6-mm-long stripline conductor; in this case, the resonance frequency of the strip structure was 0.46 GHz.

The manufactured sensor was investigated on a test bench, in which, using one pair of Helmholtz rings, sinusoidal probe (measured) magnetic fields of predetermined amplitude and frequency were created in the microstrip-structure plane. The second pair of Helmholtz rings was used to create a controllable constant magnetic bias field H_0 in the film plane. The field H_0 was oriented at the angle θ_H to the polarization direction of the high-frequency magnetic field h (see Fig. 1a). During the experiments, the sensor conversion coefficient K was measured, which was determined as the ratio of the voltage change across the detector to the probe magnetic-field value.

Figure 2 shows the change in the sensor conversion coefficient K/K_{max}, which is normalized to its maximum value, as a function of the constant magnetic bias field H_0, which is in turn normalized to the uniaxial magnetic-anisotropy field H_a.

The dependences were measured at $\theta_H = 5°$ for the orthogonal orientation of the EMA of the magnetic film relative to the polarization direction of the high-frequency microwave magnetic field of the MSR, i.e., the EMA-direction angle $\theta_a = 90°$. The constant magnetic field was swept in the forward and backward directions. It is seen that the maximum value of the conversion coefficient is observed in a field that is close to the anisotropy field, and a hysteresis is properly displayed for fields $H_0 < H_a$.

As was expected, the conversion coefficient of the studied sensor depends not only on the value of the bias field H_0 but also on its direction θ_H. Figure 3 shows the angular dependences $K(\theta_H)/K_{max}$ that were plotted at $H_0 = H_a$ for three orientation angles θ_a of the TMF easy-magnetization axis. The experimental results were normalized to the maximum conversion-coefficient value that was measured at $\theta_a = 90°$. As is

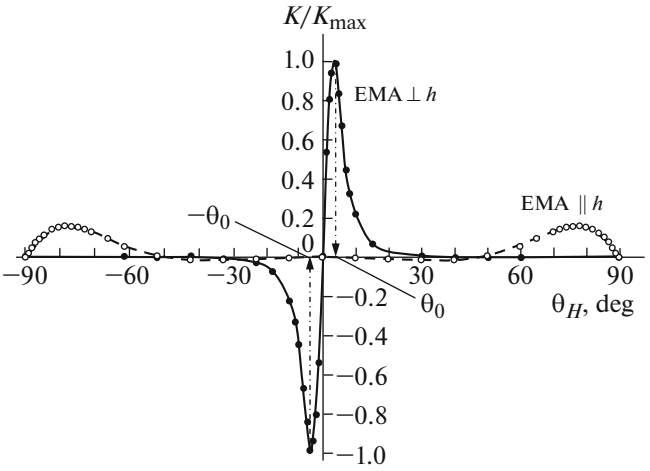

Fig. 4. The dependences of the normalized conversion coefficient of the microstrip resonator transducer on the direction angle of the bias magnetic field for two orientations of the TMF easy-magnetization axis relative to the high-frequency field polarization.

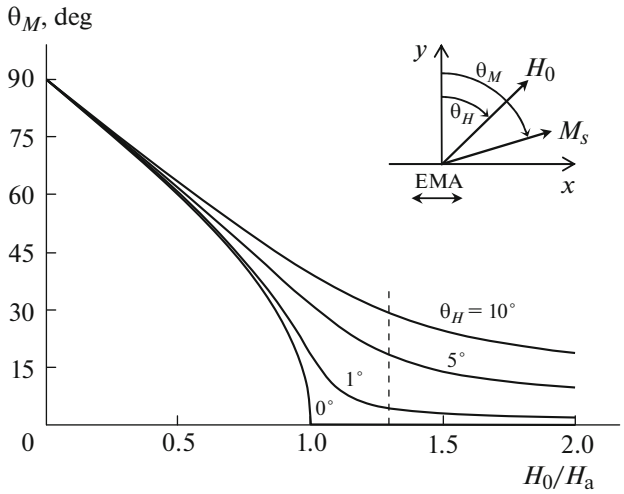

Fig. 5. The dependences of the equilibrium orientation angle of the TMF magnetic moment on the value of the bias magnetic field, which are plotted for several angles of the magnetic field orientation (figures near the curves).

seen, the sign of K changes at the point $\theta_H = 0°$, the dependences $K(\theta_H)$ are nonmonotonic in this case, and extrema are observed in them near the angles $\theta_H \approx \pm 2°$. In addition, the extreme values strongly depend on the EMA orientation angle θ_a. Identical magnitudes of K are observed at the minimum and maximum only at $\theta_a = 90°$; as the angle θ_a increases or decreases only by 5°, the value of one extremum drops by a factor of ~2, and the other slightly increases.

It should be noted that in the hysteresis region at $H_0 \le H_a$ (see Fig. 2), the equilibrium state of the TMF magnetic moment is unstable because of existing slight nonuniformities of the value and direction of the uniaxial magnetic anisotropy, which are observed in some regions over the entire film area [19]. A TMF magnetic-state instability manifests itself in the sensor detector as a comparatively high noise level, which is maximized at $H_0 \approx H_a$. However, the level of this noise quickly falls as the field increases, $H_0 > H_a$, and already at $H_0 = 1.2H_a$, magnetic noise from the TMF is virtually not detected by the sensor detector. Therefore, despite the fact that the sensor conversion coefficient decreases with an increase in the biasing field, it is desirable to use the biasing field $H_0 \ge 1.2H_a$.

Figure 4 shows the dependences $K(\theta_H)/K_{max}$ that were measured at $H_0 = 1.2H_a$ for the orthogonal (dark dots) and parallel (light dots) orientations of the TMF easy-magnetization axis relative to the polarization direction of the high-frequency pumping magnetic field. It should be noted that when the bias field H_0 increases, the character of the dependence $K(\theta_H)$ for the orthogonal orientation of the TMF easy-magnetization axis relative to h virtually does not change, but in this case, the angle θ_0 that characterizes the position of the extrema monotonically increases. As a result, at $H_0 = 1.2H_a$, the maximum and minimum of K are observed at $\theta_0 \approx 5°$ and at $\theta_H \approx -5°$ ($-\theta_0$), respectively. The magnitudes of these extrema are at least 5 times higher than the magnitudes of the extrema that are observed at $\theta_H \approx \pm 80°$, provided that h is parallel to the EMA. Therefore, in a microstrip sensor for weak magnetic fields, an operating mode when the EMA of the TMF is orthogonal to the polarization of the high-frequency magnetic field should be preferred.

Figure 5 shows the dependences of the equilibrium angle θ_M of the film magnetic-moment orientation on the magnetic bias field, which account for the nature of the existence of extrema that are observed in the dependences $K(\theta_H)/K_{max}$ for the EMA directed orthogonally to the polarization of the high-frequency magnetic field (Fig. 4). The curves are plotted on the basis of a numerical analysis of the phenomenological TMF model [20] for four bias-field orientation angles θ_H: 0°, 1°, 5°, and 10°. When the probe (measured) field is directed along the bias field, it is obvious that the conversion coefficient is proportional to the derivative of the function $\theta_M(H_0)$, which is calculated at the point that corresponds to the applied bias field. This explains the dependence of the sensor conversion coefficient on the bias-field orientation angle. In fact, the above curves clearly demonstrate that in the region $H_0 \ge H_a$ at $\theta_H = 0°$, the conversion coefficient is zero for any bias field $H_0 > H_a$. However, for any fixed value of this field, e.g., $H_0 = 1.2H_a$, which is shown in Fig. 5 with a dashed line, the optimal angle θ_H exists, which provides the maximum derivative of the function $\theta_M(H_0)$ and, consequently, the maximum sensor conversion coefficient.

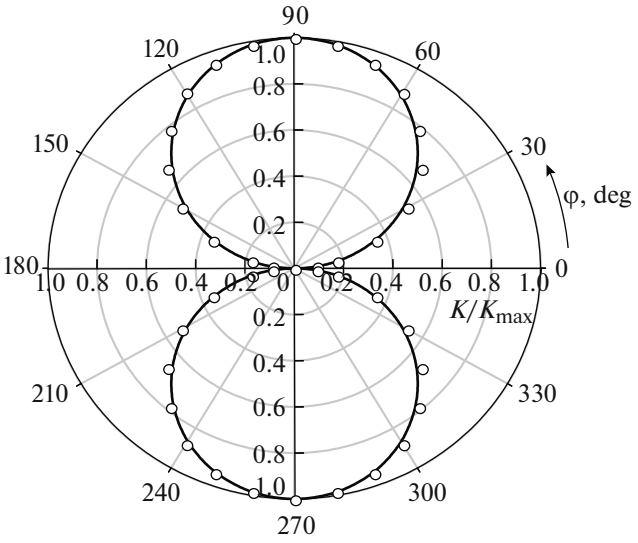

Fig. 6. The directivity pattern of the microstrip sensor of weak magnetic fields: (points) experiment and (line) calculation.

It should be noted that the conversion coefficient increases by a factor of ~4, if the probe field is orthogonal to the bias field. In this case, the maximum value of this coefficient is observed if the probe field is orthogonal to the equilibrium orientation of the TMF magnetic moment. However, when the probe field is parallel to the equilibrium direction of the magnetic moment, the conversion coefficient is zero. This fact is confirmed by the directional pattern of the investigated microstrip sensor (Fig. 6) that is measured in the sensor plane. In this case, the angle φ of the probe-field direction was measured from the equilibrium orientation of the film magnetic moment. It is seen that the measured points are in good agreement with the theoretical dependence, which is shown with a solid line in Fig. 6 in the form of two circles.

MAGNETOMETER ON RESONANCE MICROSTRIP STRUCTURES WITH THIN MAGNETIC FILMS

Two clearly pronounced extrema in the dependence of the conversion coefficient on the orientation angle of a constant magnetic bias field (Fig. 4) indicate the possibility of building a sensitive element of a magnetometer (microstrip transducer) on the basis of two identical microstrip sensors in which narrow stripline conductors are "tilted" with respect to the resonators at angles of $\pm\theta_0$ (Fig. 7). This will allow the useful signal to be doubled after summing in the operational amplifier [21].

In this case, the structural scheme of the magnetometer consists of a pump oscillator PO_{mcw} that feeds a sensitive element, which consists of two MSR-based sensors signals from which arrive at the amplitude

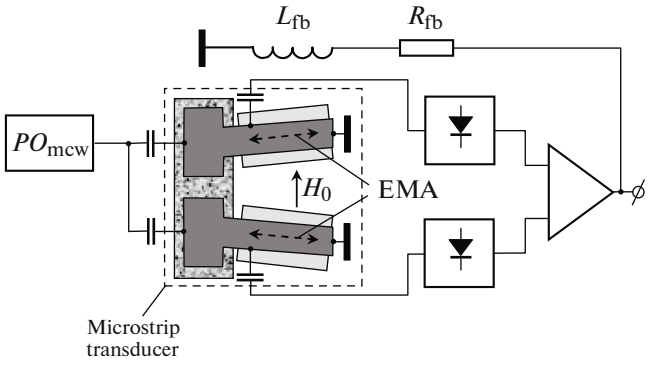

Fig. 7. The block diagram of the weak-field magnetometer.

detectors and then to an operational amplifier. In such a structural scheme, when the microwave-oscillator frequency coincides with the MSR resonance frequencies, a significant compensation of the pump-generator amplitude noise is observed, because the voltage from the sensors after the detectors are mutually subtracted at the operational amplifier. In addition, the magnetic-noise level of the sensitive element, which is built on two sensors, also decreases, evidently, by a factor of $\sqrt{2}$.

It is well known that the high long-term stability of the conversion coefficient must be provided in the magnetometer, thus substantially influencing the accuracy of determining the measured magnetic field. As a rule, this requirement is provided by the compensation measurement method with a feedback, when the sensitive element is placed inside a special coil L_{fb} (Fig. 7), which compensates for the measured-field value with a high accuracy by its magnetic field. As a result, the stability K is mainly determined by the stability of the constant of this compensation coil and the stability of the feedback resistor R_{fb} [1], which are the load of the operational amplifier, as is seen in Fig. 7.

As the compensation coil, Helmholtz rings with small dimensions were used, which make it possible to significantly reduce the shielding of the measured high-frequency magnetic fields, in contrast to solenoids that are commonly used for this purpose. It should be noted that the value of the inductance L_{fb}, also determines the frequency of the upper operating-frequency-band edge, when the reactive impedance of the coil becomes unacceptably high. However, a decrease in the inductance L_{fb} with the purpose of an additional extension of the operating frequency band will require a corresponding power increase in the compensation circuit.

In view of the directional pattern of the microstrip transducer with the TMF (see Fig. 6), it is obvious that in order to construct a vector magnetometer, it is possible to use three identical transducers with mutually orthogonal maximum-sensitivity axes. The circuit

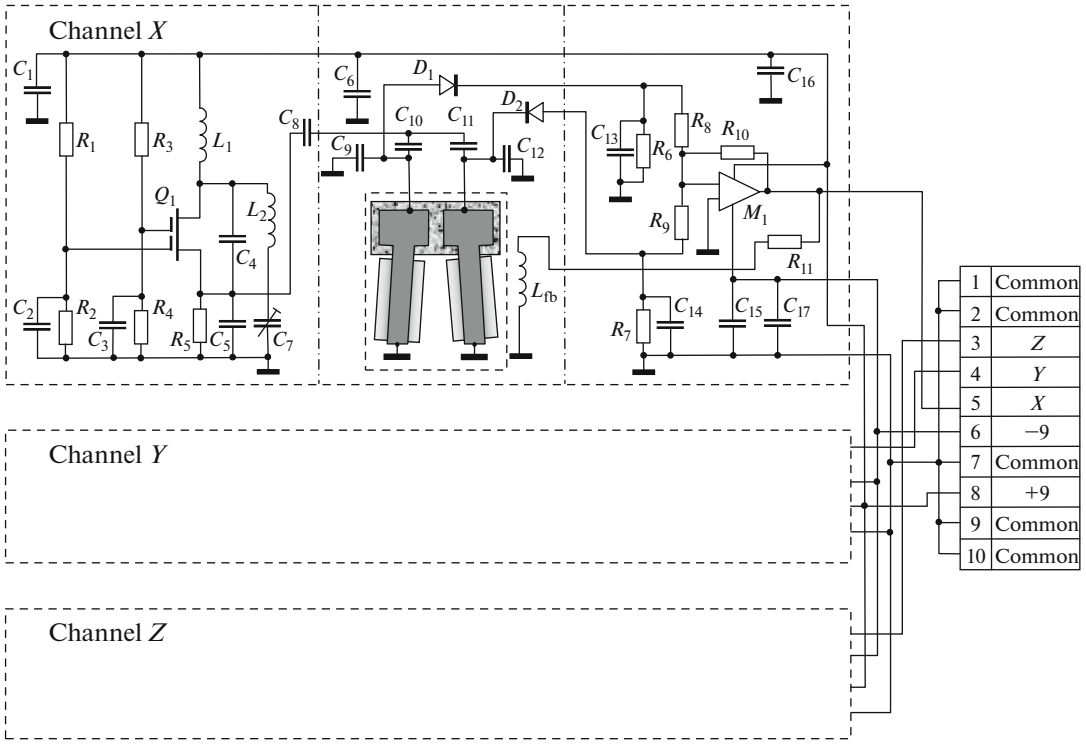

Resistors								
R_1	R_2	R_3	R_4	R_5	R_6, R_7	R_8, R_9	R_{10}	R_{11}
6.8 kΩ	470 Ω	6.2 kΩ	4.3 kΩ	100 Ω	91 kΩ	18 kΩ	1 MΩ	200 Ω
Capacitors								
C_1, C_3	C_2, C_6, C_8	C_4	C_5	C_7	C_9, C_{12}	C_{10}, C_{11}	C_{13}, C_{14}	C_{15}–C_{17}
3.3 nF	0.1 μF	2.2 pF	4.7 pF	4–30 pF	20 pF	3.3 pF	100 pF	0.1 μF

Fig. 8. The circuit diagram of the vector magnetometer of weak fields.

diagram of the vector magnetometer is shown in Fig. 8, and the nominal values of the resistors and capacitors are presented here in the table. The microwave oscillator is based on an insulated-gate field-effect transistor Q_1 (BF998), KD922 diodes were used as the detectors D_1 and D_2 diodes, and a MAX9943 chip served as the operational amplifier M_1.

As is known, permalloy films with the ~$Ni_{80}Fe_{20}$ composition, which is close to a composition with zero magnetostriction, are widely used in sensors of weak magnetic fields. The ferromagnetic-resonance (FMR) line for these films that was measured at a frequency of 2.3 GHz is $\Delta H \approx 7$ Oe, the magnetic-anisotropy field is low, $H_a \approx 5$ Oe, and the saturation magnetization is also comparatively low, $M_s \approx 860$ G. The magnetic permeability at microwaves in such films is low, but the parameters of the amplitude δH_a and angular $\delta\alpha_a$ dispersions in them are low, thus substantially reducing magnetic noises. A high permeability at microwaves is inherent to chemically deposited nanocrystalline cobalt films [22], which are promising for the use in magnetic sensors, but the "aging" problem has not yet been solved for them.

We manufactured permalloy films with the $Ni_{75}Fe_{25}$ composition for microstrip sensors. Their saturation magnetization is $M_s \approx 1100$ G, the magnetic anisotropy is $H_a \approx 8$ Oe, and the FMR linewidth measured at a frequency of 2.3 GHz is $\Delta H \approx 5$ Oe; these parameters are much better than the corresponding characteristics of $Ni_{80}Fe_{20}$ films. It is also important that in the considered design of the microstrip sensor, a significant decrease in noise from films is observed, in contrast to sensors on inductance coils. This is favored primarily by the fact that the longest edge of the TMF, which are the main noise sources, do not fall

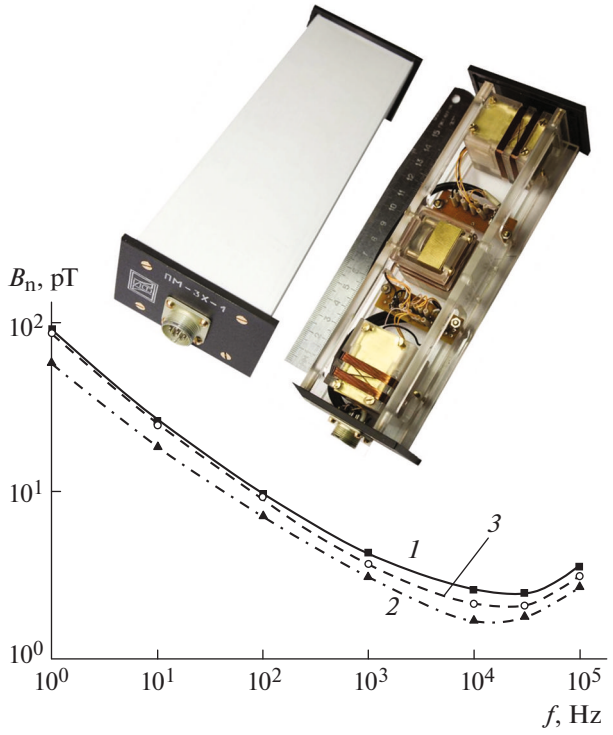

Fig. 9. The frequency dependences of the noise amplitude for the *X*-channel (*1*), *Y*-channel (*2*), and *Z*-channel (*3*) of the vector magnetometer on thin magnetic films, which were measured in a band of 1 Hz. The inset shows photographs of (on the left) the assembled magnetometer and (on the right) the magnetometer without the protecting housing.

within the region of the high-frequency magnetic fields of the MSR (see Fig. 1a); therefore, these regions do not participate in the signal formation. Second, owing to the small dimensions of the microwave sensors (~11 × 5 mm), the dimensions of the films are also small (5 × 4 mm) and, consequently, the dispersions of the characteristics of the uniaxial magnetic anisotropy δH_a and $\delta\alpha_a$ are also small [19, 22].

In addition, a scanning ferromagnetic-resonance spectrometer [23] was used to measure the distributions of the saturation magnetization, the value and direction of the uniaxial magnetic-anisotropy field, and the FMR linewidth over the entire area (60 × 48 mm^2) of the manufactured thin-film magnetic structure with a step of 1 mm. This allowed us to select areas of the magnetic structure of predetermined dimensions with the most uniform characteristics and thus to minimize the magnetic noise from the TMF.

As a result, it was established that noises of the designed magnetometer are low and are mainly due to the circuit elements: the pump oscillator, detectors, and operational amplifier. The chosen pump-oscillator frequency that coincides with MSR resonance frequencies is comparatively low (~0.46 GHz) for the sensors to operate in a mode that is close to the FMR at a relatively low bias field H_0.

One of the most important characteristics of magnetometers is the threshold of the sensitivity to the measured field, which is characterized by the noise amplitude B_n, which is usually measured in a frequency band with a width of 1 Hz. Figure 9 shows the experimental dependences of B_n on the measured-signal frequency f for each channel of the manufactured magnetometer. Noises were measured under laboratory conditions, the magnetometer was placed inside a three-layer magnetic permalloy shield with 1.0-mm-thick walls, which allowed the laboratory magnetic fields to be reduced by approximately three orders of magnitude. The magnetometer was powered from storage batteries, and the output signal was measured with a selective nanovoltmeter. As is seen, the noise amplitude of each of the three channels of the magnetometer is quite small; as the frequency increases, the noise amplitude first decreases and then begins to increase. In this case, the minima in the dependences $B_n(f)$ lie within a range of 10^4–10^5 Hz.

Figure 9 also shows photographs of the manufactured magnetometer with and without the shielding housing. The microwave-oscillator and output-amplifier boards are positioned in individual compartments of brass cases for providing their proper mutual shielding. The sensitive elements on the basis of two microstrip resonators with TMFs, the detectors, and the magnetic system for creating the bias field H_0 are positioned on a special platform, which is placed at the center of the compensating Helmholtz rings. The magnetic system that creates the bias field $H_0 \approx 10$ Oe, is built on the basis of miniature permanent magnets and magnetic circuits of soft magnetic iron.

The main performance characteristics of the developed and manufactured prototype of a vector magnetometer of weak magnetic fields are presented below:

Range of measured magnetic fields, T	10^{-10}–10^{-4}
Range of operating frequencies, Hz	10^{-1}–10^5
Deviation of mutually orthogonal axes of channels, deg, no worse	1
Conversion coefficient, mV/μT	60
Power-supply voltage, V	±9
Consumed power, W	0.5
Dimensions, mm	190 × 66 × 46
Weight, g	385

CONCLUSIONS

The design of a vector magnetometer on microstrip resonance structures with thin magnetic films was developed and investigated. The magnetometer differs from the known solutions by its simplicity, good manufacturability, and a wide band of operating frequen-

cies at a quite high threshold sensitivity, thus allowing the instrument to be used in studies of the geological structure of the earth and exploration of natural resources, including pulse electrical prospecting with artificial excitation of a medium. Owing to its small size and weight, it can be placed on light unmanned vehicles.

As compared to conventional fluxgate magnetometers on the basis of thin magnetic films, the upper edge of the operating frequencies is higher by almost one order of magnitude owing to the use of MSRs instead of oscillatory circuits on the basis of lumped capacitances and inductances. Inductance coils in magnetometers on oscillatory circuits, which are wound directly on the substrate with a TMF deposited on it, shield external high-frequency magnetic fields and therefore considerably reduce the upper edge of the operating frequencies. Thin-film sensors of the microstrip design have no such shortcomings. This opens the possibility of additionally extending their operating-frequency band, but this will primarily require a decrease in the inductance of the Helmholtz rings in the feedback path in the used compensation circuit of the magnetometer.

The directional pattern of each of the three channels of the manufactured vector-magnetometer prototype has the shape of a figure of eight in the plane of the microstrip, thus providing high-accuracy measurements of both the magnetic-field value and direction.

ACKNOWLEDGMENTS

This study was performed within the framework of the State Job of the Ministry of Education and Science of the Russian Federation for the research at the Siberian Federal University in 2014 (project no. 3.528.2014K).

REFERENCES

1. Afanas'ev, Yu.V., Studentsov, N.V., Khoreev, V.N., Chechurina, E.N., and Shchelkin, A.P., *Sredstva izmerenii parametrov magnitnogo polya* (Tools for Measurements of Magnetic Field Parameters), Leningrad: Energiya, 1979.
2. Erkan, K. and Jekeli, C., *J. Appl. Geophys.,* 2011, vol. 74, nos. 2/3, p. 142. doi 10.1016/j.jappgeo.2011.03.006
3. Ciudad, D., Díaz-Michelena, M., Pérez, L., and Aroca, C., *Sensors*, 2010, vol. 10, no. 3, p. 1859. doi 10.3390/s100301859
4. Gaffney, C., *Archaeometry,* 2008, vol. 50, no. 2, p. 313. doi 10.1111/j.1475-4754.2008.00388.x
5. Dalan, R.A., *Archaeol. Prosp.,* 2008, vol. 15, no. 1, p. 1. doi 10.1002/arp.32310.1002/arp.323
6. Vvedenskii, V.L. and Ozhogin, V.I., *Sverkhchuvstvitel'naya magnitometriya i biomagnetism* (Supersensitive Magnetometry and Biomagnetism), Moscow: Nauka, 1986.
7. Díaz-Michelena, M., *Sensors*, 2009, vol. 9, no. 4, p. 2271. doi 10.3390/s90402271
8. Aleksandrov, E.B. and Vershovskii, A.K., *Phys.–Usp.,* 2009, vol. 52, no. 6, p. 573. doi 10.3367/UFNr.0179.200906f.0605
9. Abramzon, G.V. and Oboishev, Yu.P., *Indukthionnye izmeritelnye preobrazovateli peremennykh magnitnykh polei* (Induction Measuring Transformers of Variable Magnetic Fields), Leningrad: Energoatomizdat, 1984.
10. Babitskii, A.N., Blinnikov, E.P., Vladimirov, A.G., Gitarts, Ya.I., Polyakov, V.V., and Frolov, G.I., in *Geofizicheskaya apparatura* (Geophysical Equipment), 1991, no. 94, p. 21.
11. Irons, H.R. and Schwee, L.J., *IEEE Trans. on Magnetic., Vol. Mag-8*, 1972, p. 61.
12. Bader, C.J. and DeRenzi, C.S., *IEEE Trans. on Magnetic., Vol. MAG-10.3,* 1974, p. 524.
13. Belyaev, B.A., Butakov, S.V., and Leksikov, A.A., *Russ. Microelectr.,* 2001, vol. 30, no. 3, p. 195.
14. Babitskii, A.N., Belyaev, B.A., and Leksikov, A.A., *Izv. Vyssh. Uchebn. Zaved. Fiz.,* 2013, vol. 56, no. 8/2, p. 271.
15. Babitskii, A.N., Belyaev, B.A., and Leksikov, A.A., *Izv. Vyssh. Uchebn. Zaved. Fiz.,* 2013, vol. 56, no. 8/2, p. 275.
16. Belyaev, B.A. and Serzhantov, A.M., *J. Commun. Technol. Electron.,* 2004, vol. 49, no. 3, p. 275.
17. Belyaev, B.A., Drokin, N.A., and Shabanov, V.F., *Instrum. Exp. Tech.,* 2006, vol. 49, no. 5, p. 696.
18. Belyaev, B.A., Babitskii, A.N., and Leksikov, A.A., RF Patent 2536083, *Byull. Izobret.,* 2014, no. 35.
19. Belyaev, B.A., Izotov, A.V., and Kiparisov, S.Ya., *JETP Lett.,* 2001, vol. 74, no. 4, p. 226.
20. Belyaev, B.A. and Izotov, A.V., *Phys. Solid State,* 2007, vol. 49, no. 9, p. 1731.
21. Babitskii, A.N., Belyaev, B.A., Skomorokhov, G.V., Izotov, and Galeev, R.G., *Tech. Phys. Lett.,* 2015, vol. 41, no. 4, p. 324.
22. Belyaev, B.A., Izotov, A.V., Kiparisov, S.Ya., and Skomorokhov, G.V., *Phys. Solid State*, 2008, vol. 50, no. 4, p. 676.
23. Belyaev, B.A., Izotov, A.V., and Leksikov, A.A., *IEEE Sensors J.,* 2005, vol. 5, no. 2, p. 260.

Translated by A. Seferov